

P12.7 EXPLORATION OF A MODEL RELATING ROUTE AVAILABILITY IN EN ROUTE AIRSPACE TO ACTUAL WEATHER COVERAGE PARAMETERS[†]

Brian D. Martin*, James Evans, and Richard DeLaura
 MIT Lincoln Laboratory
 Lexington, Massachusetts

1. INTRODUCTION

A major concern in contemporary traffic flow management (TFM) is improving decision making when severe convective weather (Wx) impacts en route sectors throughout the National Airspace System (NAS). The FAA is currently seeking to reduce these convective weather delays through the use of multi-hour (e.g. 4 and 6 hour) Wx forecasts coupled with strategic planning by the FAA traffic flow managers and airline personnel to determine how en route traffic should be rerouted so as to avoid sector overloads and minimize the magnitude of the delays that occur [Huberdeau and Gentry (2004)]. One of the major challenges in the strategic planning process is the difficulty in converting the convective weather forecasts into forecasts of en route sector capacity.

In this study, we explore the development of a model that can be combined with forecast validation data to translate probabilistic convective weather (Wx) forecasts into forecasts of a surrogate for sector capacity - the fraction of jet routes that would be blocked- within an en route sector.

The principal objectives of this exploratory study were to:

- (i) develop a methodology for relating route blockage to Wx parameters that could reasonably be generated by a contemporary convective weather forecast. Examples of the Wx parameters are the fractional coverage of high reflectivity radar returns, fractional coverage of high radar echo tops, and the type of convective storms, and

- (ii) apply the methodology to 10 en route sectors from the highly congested Great Lakes and Northeast Corridors using 20 Corridor Integrated Weather System (CIWS) Wx data sets

Given that there is no generally accepted model for the number of aircraft that can be handled by a controller (or, an en route sector) as a function of coverage by Wx¹, this study has focused on a closely related metric which is the fraction of normal jet routes within a sector that are not blocked by the convective weather.

While it is currently difficult to forecast several hours in advance the exact locations of Wx cells precisely, we postulate that it is possible to forecast with some appreciable skill, the broad characteristics of the storms that are likely to occur in a region – the percent of likely sector coverage by high reflectivity cells, the likely echo tops spatial distribution, the types of storms likely to occur, and given an organized line storm type, the likely orientation.

We develop separate models for each ATC sector that relate the RB for that sector to the Wx storm characteristics within that sector. This is because:

1. the structure and spatial orientation of the routes within a sector can differ greatly between sectors (as is shown in section 2.3), and
2. geographical factors may cause convective storms to have preferred orientations in different regions

For each time sample of the Wx spatial pattern in each of the 10 en route sectors, the route blockage (RB) is calculated using a modified version of the route blockage algorithm for the Route Availability Planning Tool (RAPT) which is currently in operational use for departures from the

[†]This work was sponsored by the National Aeronautics and Space Administration (NASA) under Air Force Contract FA8721-05-C-0002. Opinions, interpretations, conclusions, and recommendations are those of the authors and are not necessarily endorsed by the United States Government.

*Corresponding author address: Brian Martin, MIT Lincoln Laboratory, 244 Wood Street, Lexington, MA 02420-9185; e-mail: bmartin@ll.mit.edu

¹ Studies of cognitive complexity in air traffic control are germane to determining the effective capacity of a sector in convective weather. (Histon, et. al., 2002) discuss the impact of convective weather on cognitive complexity within a sector in the Boston ARTCC (ZBW).

New York City airports [DeLaura and Allan (2003)].

We then form a data base consisting of Wx parameters and computed RB for each ATC sector as a function of time. Statistical classification techniques are used to generate a model that predicts the RB in an ATC sector as a function of the Wx parameters. The performance of the models in correctly predicting the RB given a set of Wx parameters has been evaluated quantitatively on a set of measured Wx-RB data samples that are different from the set of measured Wx-RB data samples used to develop the models.

The paper proceeds as follows. In section 2, we show how the model developed here can be used to translate probabilistic convective weather forecasts into forecasts of route blockage within a sector as well as describing the details of the data processing (i.e., meteorological data, en route sector data, the route blockage algorithm and the statistical classification techniques). Section 3 presents results of analyzing the initial data sets. Section 4 summarizes the results and section 5 makes suggestions for future studies.

2. DATA AND METHODOLOGY

2.1 Relationship of Route Blockage Model to a Forecast of Route Blockage

From elementary probability theory, the probabilistic forecast of RB given a probabilistic weather forecast, F, can be determined from:

$$P(RB|F) = \int P_1(RB|\underline{W}_c) P_2(\underline{W}_c|F) d\underline{W}_c \quad (1)$$

Where:

$P(RB|F)$ is the probability distribution of RB in an ATC sector given a Wx forecast with parameters F (i.e., the probabilistic forecast of RB).

$P_1(RB|\underline{W}_c)$ is the probability that route blockage is RB given that actual Wx parameters are \underline{W}_c (a vector). This paper discusses the development of a model for $P_1(RB|\underline{W}_c)$.

$P_2(\underline{W}_c|F)$ is the probability (density) that the actual Wx parameters are \underline{W}_c given that the Wx forecast of parameters F was made. The model for $P_2(\underline{W}_c|F)$ is developed from meteorological validation of the probabilistic forecast [see, e.g., (Mahoney, et. al., 2002)]

By integrating the product of the P_1 and P_2 terms with respect to the continuous variable \underline{W}_c , one obtains the probabilistic forecast of RB conditional on F. An advantage of determining $P(RB|F)$ by the above approach as opposed to empirically assessing the actual RB for many issued forecasts, is that only meteorological validation needs to be redone [that is, the model for $P_2(\underline{W}_c|F)$ is regenerated] when the forecasts are changed. Additionally, the route blockage model [$P_1(RB|\underline{W}_c)$] can be used for many different probabilistic forecast algorithms as long as the various forecasts generate estimates of the weather parameters, \underline{W}_c , used for $P_1(RB|\underline{W}_c)$.

2.2 Meteorological Data

For this Wx-RB modeling study, 20 Wx events were examined, each having significant operational impact within the coverage region of the CIWS. Table 1 provides the starting date for each of the 20 Wx events, with associated storm organization, Wx types, and impacted Air Route Traffic Control Centers (ARTCCs). Weather events were chosen based on widespread impact on the National Airspace System (NAS), diversity of Wx type, and diversity of vertical structure within individual storms.

The Wx parameters include storm intensity, type, and vertical extent, orientation of line storms, and dominant Wx type within an ATC sector. These quantities are derived from the CIWS output fields of the high-resolution vertically integrated liquid (VIL) product, the Regional Convective Weather Forecast (RCWF) Wx classification product², and the CIWS Echo Tops product respectively. More complete information on CIWS and its weather products is provided in the CIWS operational benefits report [Robinson, et. al., (2004)] and the CIWS product description report [Klinge-Wilson and Evans (2005)].

Intensity of a thunderstorm is characterized by the CIWS high resolution VIL. CIWS VIL mosaics are created at a temporal resolution of 5 minutes with geographic location and intensity of precipitation mapped to a 1-km resolution horizontal grid. Figure 1 shows an example of thunderstorm intensity as portrayed by the CIWS NEXRAD VIL product. The strongest portions of thunderstorms are colored in red and correspond to VIP (Video Integrator Processor) level-6 intensities.

²The Wx classification product is generated internally by the RCWF algorithm that is not provided currently to the ATC users of the RCWF.

The classification of precipitation into Wx type is an internal feature of the CIWS Regional Convective Weather Forecast (RCWF) algorithm. Wx type classification is used to optimize the performance of the RCWF forecast. The RCWF classification technology defines six Wx types differing in size and motion characteristics. Five RCWF Wx types were available at the time this

study was complete and include "line", "small cell", "large cell", "stratiform precipitation", and "embedded". The 6th Wx type "weak cell" was added in summer of 2004. Figure 2 is a flow diagram of the RCWF Wx classification algorithm and visual representation of the five Wx types used in this study.

Table 1

Case data for 20 active Wx days used in the Wx-RB study. Cases were chosen primarily from the 2003 Wx season. Information includes date, overall Synoptic organization (organized, unorganized, or both), Wx type, and impacted ARTCCS.

Date	Organization	Wx Type	Impacted ARTCCS
020822	Both	Line, Embedded, Isolated	ZAU,ZOB,ZNY,ZBW
030319	Organized	Line, Embedded	All CIWS ARTCCS
030420	Organized	Line, Isolated	ZAU,ZOB,ZNY
030501	Both	Line, Isolated, Embedded	All CIWS ARTCCS
030505	Unorganized	Embedded	All CIWS ARTCCS
030509	Both	Isolated, Embedded	ZAU,ZID,ZOB,ZDC,ZNY
030531	Both	Line, Embedded, Isolated	ZID,ZOB,ZDC,ZNY,ZBW
030608	Organized	Line, Embedded	ZAU,ZID,ZOB,ZDC,ZNY
030611	Organized	Line, Embedded	All CIWS ARTCCS
030614	Both	Line, Isolated	All CIWS ARTCCS
030626	Organized	Line, Embedded	ZAU,ZID,ZOB
030706	Organized	Line, Isolated	All CIWS ARTCCS
030709	Organized	Line, Isolated	ZAU,ZID,ZOB,ZDC,ZNY
030721	Organized	Line, Isolated	All CIWS ARTCCS
030731	Both	Line, Isolated, Embedded	ZAU,ZID,ZOB,ZDC
030804	Both	Line, Isolated	All CIWS ARTCCS
030822	Both	Line, Isolated	ZID,ZOB,ZDC,ZNY,ZBW
030826	Both	Line, Isolated, Embedded	All CIWS ARTCCS
030829	Both	Line, Isolated, Embedded	All CIWS ARTCCS
030901	Organized	Line, Isolated, Embedded	ZAU,ZID,ZOB,ZDC,ZNY

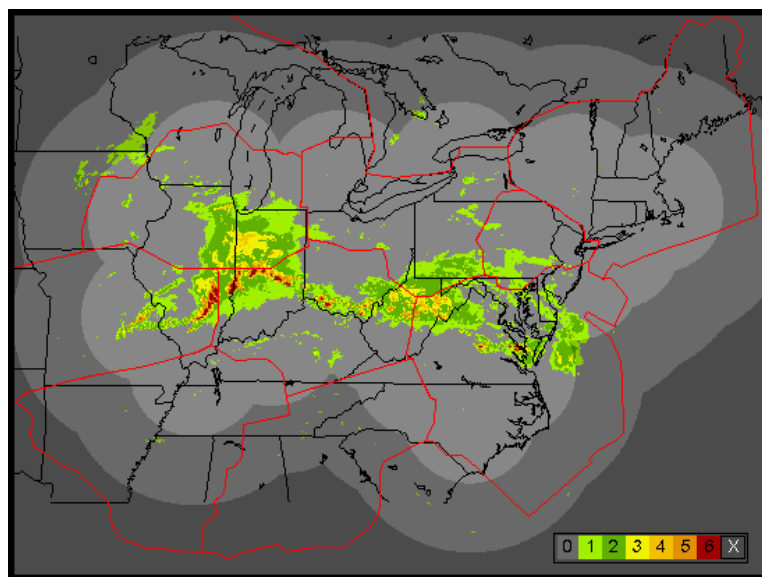


Figure 1. Extent of the CIWS domain and the corresponding NEXRAD radar coverage. Best radar coverage within the domain is indicated by the lightest shade of grey. Wx on 10 May 2003 – 16:07:28 UTC provides an example of the 6-level intensities available through the CIWS NEXRAD VIL product. Level-6 intensities in the VIL product are colored red and represent the strongest thunderstorm cores. Bright red contours are the ARTCC boundaries.

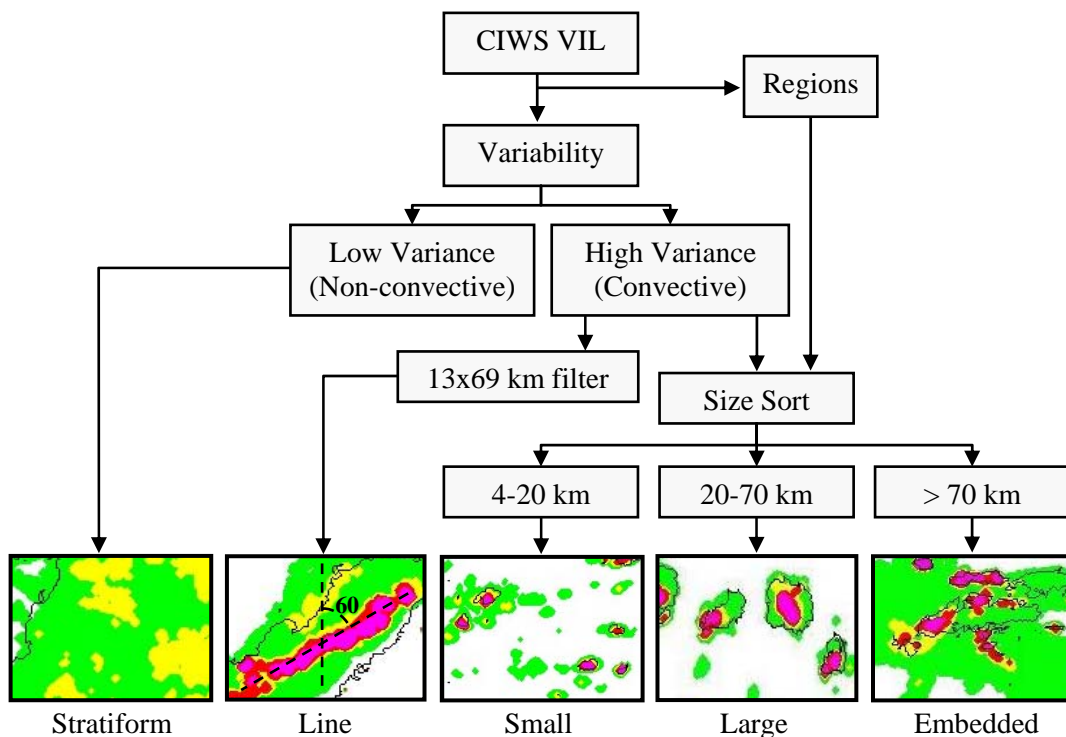


Figure 2. Flow diagram of the CIWS RCWF Wx type classification algorithm. Lower images provide a visual representation of the five Wx types classified by the RCWF algorithm.

The spatial pattern of the vertical extent of thunderstorms is characterized by the CIWS Echo Tops mosaic product. The Echo tops data used in this study have a temporal resolution of 5-minutes and are mapped to a 1-km horizontal grid. [Rhoda, et. al. (1999, 2002), [Robinson, et. al., (2004), and DeLaura and Evans (this conference)] have shown that the vertical structure of a storm relative to aircraft altitude is a very important factor in determining whether a convective storm will block a route in en route space.

Given that the intent of the study is to provide a model that can be used for probabilistic Wx forecasts, the spatial distribution of Wx within an ATC sector is characterized by the fractional Wx coverage and parameters associated with that coverage. Fractional coverage is defined as the area Wx covers with respect to the total area of the ATC sector and will be expressed as a percentage. The Wx parameters used were:

1. Fractional Wx coverage of VIL greater than or equal to VIP level 1 (*/level1+wx*)
2. Fractional Wx coverage of VIL greater than or equal to VIP level 3 (*/level3+wx*), that is the convective elements.
3. Fractional coverage of Wx with echo tops greater than or equal to 25kft (*/etops25+*)
4. Fractional Wx coverage of VIL greater than or equal to VIP level 3 with echo tops greater than or equal to 25kft (*/3andet25*)
5. Fractional coverage of Wx classified as type line (*/line*)
6. The average azimuth orientation of the line types that fractionally cover a sector (*orientation*)
7. Fractional coverage of Wx classified as type small (*small*)
8. Fractional coverage of Wx classified as type large (*large*)
9. Fractional coverage of Wx classified as type stratiform (*stratiform*)

10. Fractional coverage of Wx classified as type embedded (*embedded*)
11. Dominant Wx type of the classified fractional coverage within an ATC sector (*wx-type*)

2.3 Air Traffic Control Sector Data

Ten ATC sectors have been chosen for the Wx-RB modeling study. Figure 3 shows the ATC sectors of interest chosen due to their differences in geographic location, size, route orientation, and route complexity. These ATC sectors include high traffic areas seen as major choke points within the Indianapolis (ZID) and Cleveland (ZOB) centers, major north-south/south-north transit routes within sectors of the Washington (ZDC) center, and one of the Chicago (ZAU) center sectors responsible for transcontinental air traffic over the mid-west. Within the 10 ATC sectors, a total of 60 high jet routes (seen in figure 3, left) comprise the route data made available for Wx-RB modeling study.

2.4 Calculation of Route Blockage for ATC En-route Sector (RB)

Given the route information and the measured meteorological quantities for a time sample provided by CIWS, the route blockage is estimated for each route within a sector. The RAPT route blockage algorithm [DeLaura and Allan, 2003] was adapted for an en-route ATC sector by:

- Considering all high jet routes bounded by a given ATC en route sector.
- Computing separate blockage computations based on Wx intensity and Wx vertical extent for the affected portions of each route within a sector.

Summing the maxima of these separate blockage computations along each route and dividing by the total number of routes within the ATC en route sector. This determines the sector's average route blockage. This fraction of routes blocked within the domain of an ATC en route sector is expressed as a percentage (0-100%) and is the quantity denoted as RB. Figure 3 - right provides a visual example of the calculated ATC sector RB given a snapshot of CIWS Wx data during an event that had significant impact on the NAS.

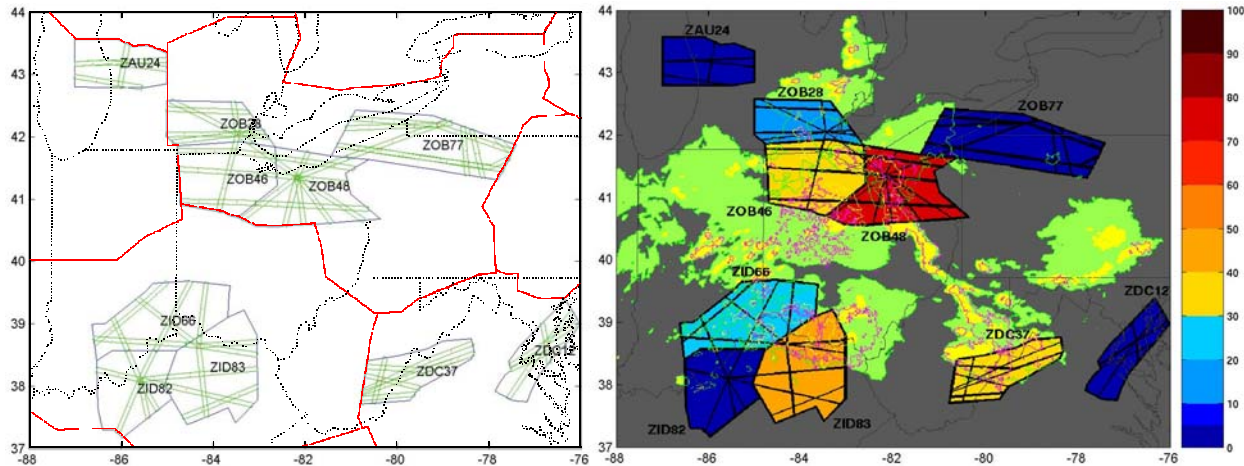


Figure 3. Left - 10 ATC sectors chosen within the NAS for there differences in geographic location, size, route orientation, and route complexity. Represented are high altitude en route sectors within the Indianapolis Center (ZID), Cleveland Center (ZOB), Washington Center (ZDC), and Chicago Center (ZAU). Principal high altitude jet routes in the various en route sectors are plotted in green. Right – Example of RB during a significant Wx event. Sectors are colored based on RB percentage as indicated by the colorbar to the far right. Wx depicted in green represents VIL between VIP levels 1 and 2, Wx depicted in yellow represents VIL of at least VIP level 3. Magenta contours bound echo tops of at least 32 kft.

From the 20 active Wx days selected for the Wx-RB modeling study, RB scores have been computed for the 10 chosen ATC sectors at a temporal frequency of 5-minutes matching the CIWS data output interval. This resulted in 6,798 sets of Wx parameters and RB scores being calculated for each ATC sector. The combined Wx-parameter / RB data sets constructed for each ATC sector were then edited to remove time samples absent of precipitation. The edited data were presented to Lincoln Laboratory's LNKnet Practical Pattern Classification software for the modeling of RB.

2.5 Pattern Classification Algorithms Used to Develop Predictive Model for Route Blockage

LNKnet software has been developed to simplify the application of statistical, neural network, and machine learning pattern classifiers [Lippmann and Kukolich (2004)]. LNKnet has been used to perform two functions:

1. to determine the explanatory power of the derived Wx parameters over the variation seen in RB. This is accomplished through the LNKnet feature selection process.

2. to construct and test a model of RB as a function of the best combination of explanatory Wx parameters. This combination of parameters produces the lowest – statistically significant RB classification error during training of the model.

Based on the recommended methodology described in the LNKnet documentation, 80% of the edited data for each sector was used for the purposes of training classification routines and the remaining 20% was reserved for testing of the developed classifiers for that sector.

Of the large number of classification routines made available through the LNKnet software package, we found that best performance for our study consistently was a K-Nearest Neighbor classifier (KNN). The KNN routine employs a Euclidian distance formula to construct complex decision regions for classification.

A requirement of the LNKnet software package is that the dependent variable (i.e., RB) be quantized into a set of classes. For this exploratory phase of the development of a Wx-RB model, the 6,798 Wx parameter-RB data points per ATC sector required a relative coarse discrete binning of the dependent variable RB. Bins of [0-20%), [20-40%), [40-60%), [60-80%), and [80-100%] were used to model RB as a function of the measured Wx parameters.

3. RESULTS

3.1 Statistical Distribution of RB and Wx Parameters

With each Wx parameter combined over all ATC sectors, Figure 4 shows the sample probability distributions (PDs) for each Wx parameter used in the Wx-RB modeling study. Excluded from the figure is *orientation*, a parameter specific to Wx coverage associated with type *line*. The PDs are derived from a data set where “Wx free” measurements were deleted. The resulting edited data is made up of 26,955 measured Wx instances over all ATC sectors.

An important feature to notice is the non-Gaussian, steep Gamma-like distribution of each Wx parameter involving fractional Wx coverage. The majority of the data sampled is heavily skewed toward low fractional coverage within an

ATC sector. When examining the data on a sector by sector basis, these distributions shift slightly depending on the coverage area of the sector and data density, but retain the same skewness. Of the *wx-type* parameter, relative frequency of occurrence is highest for storm type line. The *wx-type* “none” of the distribution is associated with benign-low reflectivity Wx that the RCWF Wx type classification algorithm does not assign a type. These events contribute to a zero or near zero RB percentage.

RB distributions for each ATC sector are reflective of the Wx parameter distributions seen in Figure 4. Given that low fractional coverage dominates the 20 day Wx sampling effort, lower percentages make up the bulk of the RB data of each sector. Figure 5 provides the discrete PDs of RB for the ten ATC sectors as a function of the edited data set. What is apparent is that for each ATC sector, patterns contributing to the 0-20% RB have been heavily sampled in comparison to the others.

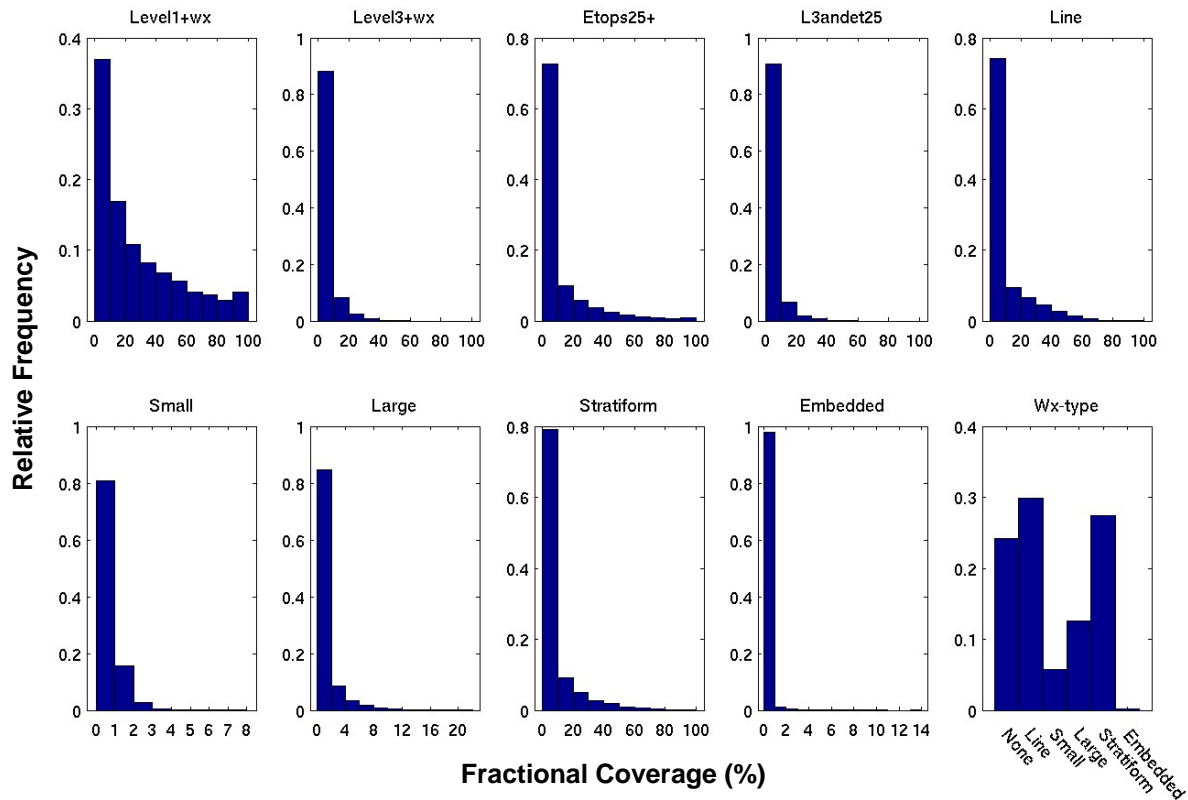


Figure 4. Probability distributions (PDs) of the Wx parameters derived for WX-RB modeling (orientation parameter specific to line excluded). The plot in the lower right corner shows the PD of the categorical parameter Wx-type. Notice that x and y axes have limits that differ in range from plot to plot.

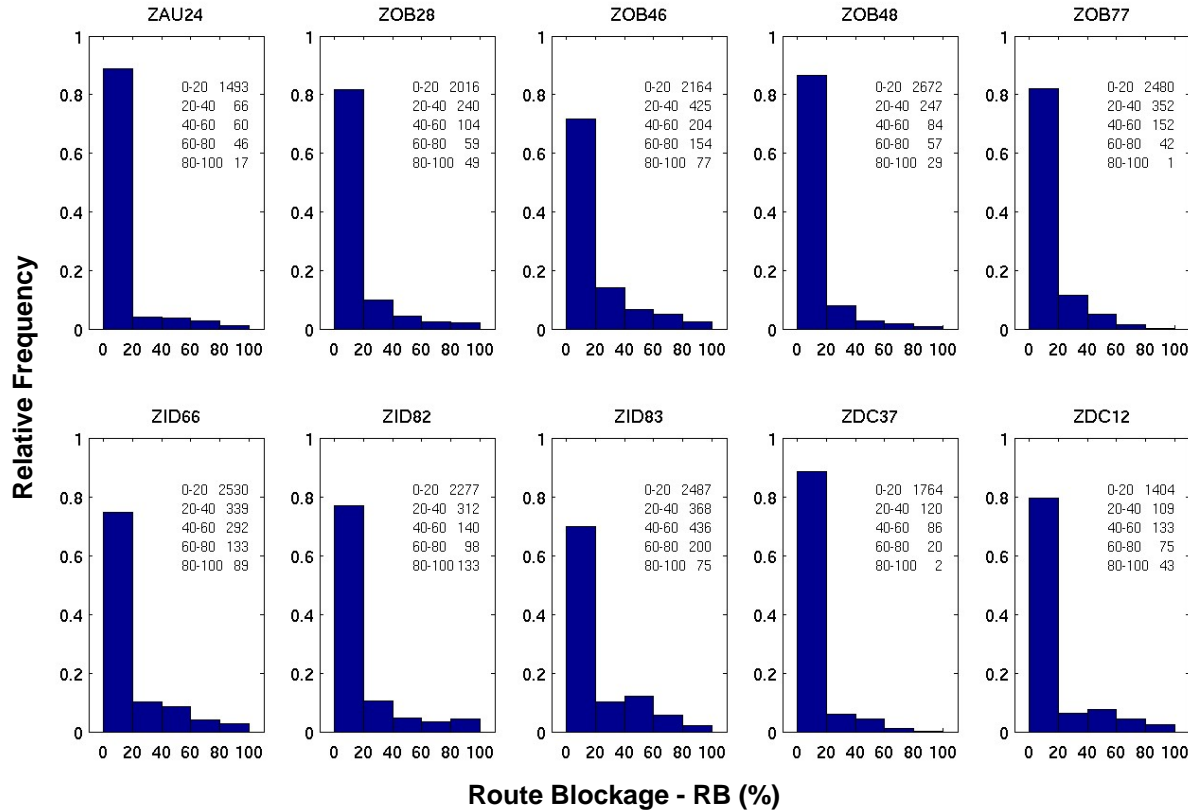


Figure 5. Discrete probability distributions of RB for each ATC sector. The legends represent histogram counts for the discrete bin intervals of RB for each ATC sector.

3.2 Differences in Sector RB given “Similar” Weather Events

As seen in section 2.3, ATC sectors differ in spatial size, they also differ in route complexity, and route orientation. An important postulate of this study has been that for similar Wx events, the impact of such events will differ from ATC sector to ATC sector. Not only will the impact depend upon the characteristics of a sector, but impact will depend on the local variability in the spatial pattern of Wx as well³. To demonstrate how the route blockage impact within the ten ATC sectors under study differ for “similar” weather events, a sub-sample of the data has been made consisting of Wx events similar in Wx type, sector fractional coverage, and vertical extent.

Figure 6 represents the RB PDs for each ATC sector given a sub-sample of 1,652 recorded impact instances of *wx-type* line. Each

wx-type line in the sub-sample holds a general east-west orientation (between 70° and 110° azimuth), with a fractional coverage of between 30% and 50%, and *etops25+* exceeding a fractional coverage of 10%. These features of *line* type are typical of medium intensity line storms.

Distributions of RB differ from sector to sector given the specific type of line storm events. The RB of ZOB28, ZOB48, ZID66, ZID82, and ZDC37 are skewed toward lower blockage percentages. ZID83 has a RB PD that weakly resembles a Gaussian distribution. The ZID83 mean RB is 46% with $\sigma = \pm 21\%$. ZAU24, ZOB77, and ZDC12 have relatively flat RB distributions. ZOB46 appears multimodal with local maxima at the [20-40%) and [60-80%) intervals. While this line storm sub-sample is limited to 1652 occurrences, differences in the distributions emphasize that estimates of capacity degradation resulting from Wx are directly attributable to ATC sector size, route orientation, and regional effects on line storm characteristics.

³ For example, some sectors (e.g., ZOB77 and ZAU24) are near a major lake while others (e.g., ZDC37) contain mountains.

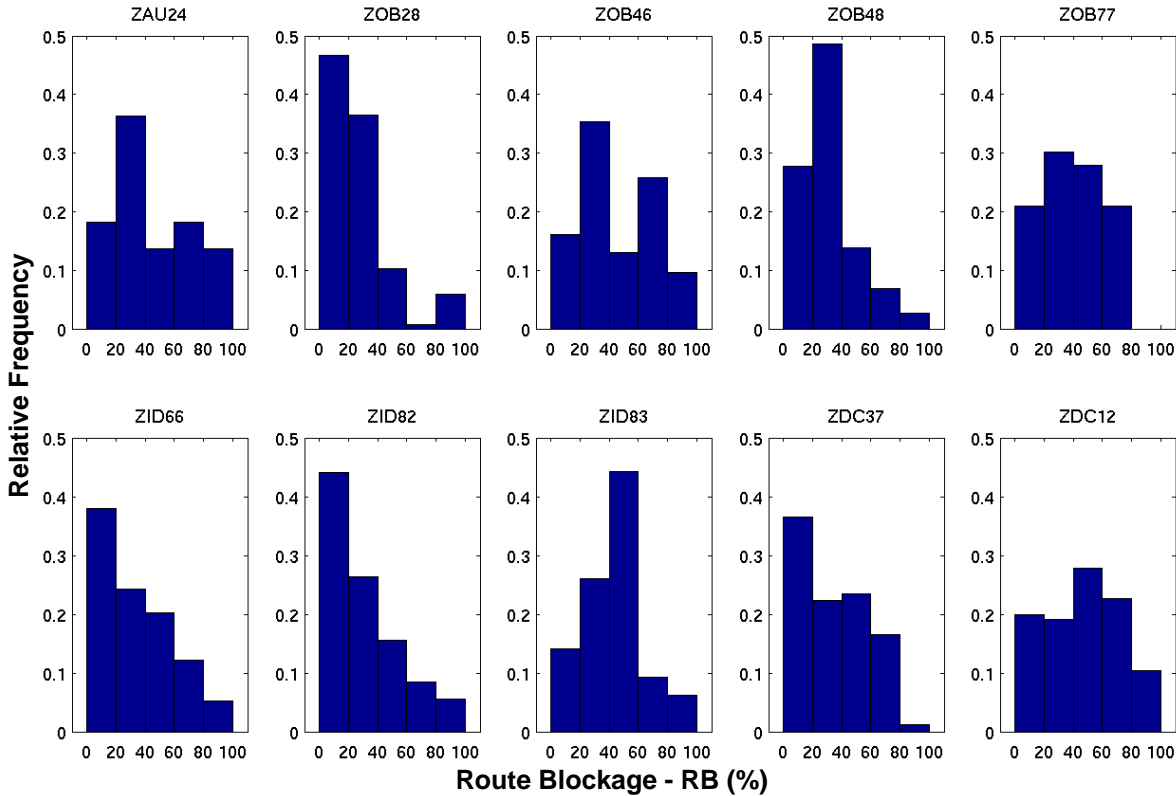


Figure 6 Probability distributions of RB for each of the 10 ATC sectors given a sub-sample of storm type line. Distributions of blockage differ from sector to sector as a result of their differences in size, route complexity, orientation, and regional effects on storm characteristics.

3.3 Blockage Sensitivity to Criteria Used in Determining Blockage

Another important issue is the role of the echo tops in addition to VIL in determining RB. The CCFP validation studies to date [Mahoney, et al. (2002) and Mahoney (2004)] and the Enhanced Traffic Flow Management System (ETMS) principally consider only storm reflectivity in determining regions of significant Wx. In Figure 7, we compare two different calculations of RB, one that utilizes 2-D information available through storm reflectivity and another that considers both storm reflectivity and the 3-D representation of Wx made available through the CIWS echo tops product.

We see that the consideration of storm echo tops as well as storm reflectivity reduces the estimated loss of capacity due to Wx by roughly a factor of two (as measured by the two RB calculations). There are a number of individual cases (those on the main diagonal) where the consideration of echo tops makes no difference. Additionally, since echo tops greater or equal to 36 kft increase the blockage score, there are

some cases where the consideration of echo tops lead to a greater route blockage. However, overall, it is clear that the consideration of echo tops in determining route blockage in en route airspace is very important.

3.4 Classification Results

LNKnet feature selection has revealed that when modeling RB as a function of each Wx parameter separately, parameters associated with Wx vertical extent into an ATC sector (i.e., *etops25+* and *l3ander25*) have the greatest explanatory power over the variability seen in RB followed by the Wx parameter associated with high intensity Wx (*/level3+wx*). This result is expected in that the blockage calculation uses echo-top heights to aggressively increase or decrease RB using the various measures of VIL. While parameters associated with Wx vertical extent and intensity generally provide the highest explanatory power of the variability seen in RB, results show, that in each case, using a combination of multiple Wx parameters significantly improves classification results.

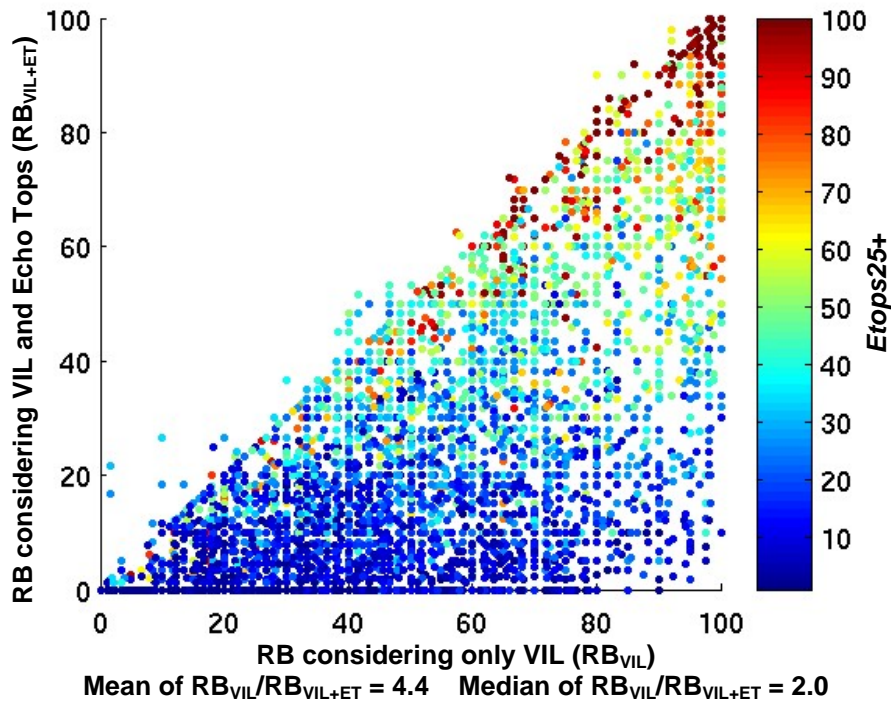


Figure 7. Comparison of ATC sector RB considering only storm reflectivity versus RB considering both storm reflectivity and echo tops. The percentage of routes blocked if one considers only storm reflectivity is about twice that determined considering both storm reflectivity and echo tops. Data points above the diagonal indicate where echo tops boost the RB calculation. The scatter plot is colored based on fractional coverage of the Wx parameter etops25+.

With the exception of CIWS, the majority of forecast systems display both probabilistic and deterministic fields of Wx intensity from a 2-D perspective, without much information on Wx vertical characteristics or type. This 2-D perspective is simulated in this study by the actual coverage of high intensity VIL within an ATC sector (i.e., level3+wx). Below in Table 2 is an error summary comparing KNN classifications of RB that utilize the best combination of Wx parameters to RB classifications based solely on 2-D information provided by the level3+wx Wx parameter. The comparison illustrates the importance of including a combination of Wx parameters that provide the 3rd dimension of vertical extent as well as some information on regional storm characteristics. In one comparison, a nearly 5:1 reduction in the overall error is realized by utilizing the best combination of Wx parameters (ZDC37).

Error statistics show that for the heavily sampled RB interval of [0-20%), errors in classification were held to less than five percent for all ten sectors (Table 3).

Classification errors are typically larger for the middle range RB intervals of [20-40%), [40-60%), and [60-80%) in comparison to the errors calculated for the tail RB intervals of [0-20%) and [80-100%). Input spaces attributed to these mid intervals overlap and are heavily mixed, contributing to the higher calculated error rate of the KNN classifier. For KNN, mid RB intervals are less distinguishable from their neighbors of a different class, the result of possibly over fitting the data to a 20% interval at these middle RB ranges.

While sparse, patterns associated with the high RB interval of [80-100%) exhibit good classification success when even a small number of patterns are made available for training and testing. Patterns related to the [80-100%) RB reside in an input space that allows them to be distinguished well from the lower RB intervals. ZAU24 was the only sector that held an [80-100%) error greater than 25% (at 66.7%). Data for ZAU24 at RB of [80-100%) is highly scattered in comparison to those sectors that exhibit good classification at this interval. Sparseness of input patterns also reveals that for ZOB77 and ZDC37, no patterns associated with the [80-100%) RB interval were available for testing (see related histograms in Figure 5).

Table 2

Comparison of classification errors of a KNN RB model based on the single parameter level3+wx (row 2) to that of a KNN RB model based on the best combination of Wx parameters as determined through feature selection (row 3). Row 4 is the level3+wx to best combination ratio. In all 10 ATC sectors, the best combination of Wx parameters holds the lowest classification error. Bottom row indicates combined number of samples collected for training and testing.

ATC Sector	ZAU24	ZOB28	ZOB46	ZOB48	ZOB77	ZID66	ZID82	ZID83	ZDC12	ZDC37
Level3+wx Error %	14.63	18.33	24.92	12.52	15.81	31.5	31.69	41.07	19.37	23.93
Best Combination Error %	5.67	12.22	9.97	4.72	7.15	10.1	13.22	10.83	13.68	5.04
Improvement Ratio	2.58	1.50	2.50	2.65	2.21	3.12	2.40	3.79	1.42	4.75
Total # of Samples	1682	2468	3089	3027	3383	2960	3566	1992	1764	1992

Table 3

Per ATC sector classification errors for the discrete RB intervals. Bottom row indicates combined number of samples collected for training and testing (see figure 5 for per sector RB histograms).

ATC Sector	ZAU24	ZOB28	ZOB46	ZOB48	ZOB77	ZID66	ZIB82	ZID83	ZDC12	ZDC37
[0-20%) Error %	1.01	4.96	4.63	1.50	3.25	1.78	3.30	2.62	4.27	1.42
[20-40%) Error %	53.85	58.33	27.06	20.41	27.14	38.81	50.60	38.36	52.38	30.43
[40-60%) Error %	16.67	40.05	22.51	43.75	23.33	34.48	71.43	28.74	57.69	41.18
[60-80%) Error %	55.56	36.36	23.33	36.36	12.50	38.46	42.11	22.00	53.33	25.00
[80-100%) Error %	66.67	0.00	6.67	0.00	NAN	17.65	15.38	20.00	25.00	NAN
Total Error %	5.67	12.22	9.97	4.72	7.15	10.10	13.22	10.83	13.68	5.04
Total # of Samples	1682	2468	3089	3027	3383	2960	3566	1992	1764	1992

While the KNN routine is able to classify RB in the data that it is presented with relatively low error rates, as with the other PPC algorithms examined in this study, its effectiveness is significantly limited by the number and diversity of the input data. The expected functional dependency of RB on fractional coverage differs significantly from what is expected given the viewpoint of conceptual arguments. RB models should exhibit a monotonic increase as, say two Wx parameters, *etops25+* and *level3+wx* increase. This expected functional dependency has yet to be achieved but an effort is currently underway to significantly increase the amount of input data presented to the PPC algorithms. With that said, the promising results of this exploratory Wx-RB study do show that the surrogate for sector capacity RB can be modeled as a function of Wx parameters.

4. CONCLUSIONS

This exploratory Wx-RB modeling study is the first attempt to relate an operational measure of RB within an ATC sector to convective weather parameters that could reasonably be generated by a multi hour probabilistic convective weather forecast algorithm. The Wx parameters used account for Wx intensity, organizational type, and vertical extent.

Calculation of RB considering vertical extent as represented by echo tops as well as storm reflectivity reduces the estimated loss of capacity due to convective weather by roughly a factor of two. Our findings suggest that parameters derived from storm height (such as *etops25+* and *I3ande25*) are key in determining sector capacity loss due to convective weather. Capacity loss will be significantly reduced by considering echo tops as well as storm reflectivity in assessing the operational impact of convective weather.

Results show that, based on the data collected from 20 active convective days across the CIWS domain, modeling of ATC sector impact has been accomplished reasonably well for the relatively low (less than 20%) route blockage events. Apparent success for these events is due to the relatively large number of convective events with low route blockage. The number of experimental low blockage events (RB less than 20%) is an order of magnitude larger than the combined number of sampled higher blockage events (RB greater and equal to 20%).

While results are promising, the statistical pattern classification models developed for the higher route blockage events are clearly in need of a substantially larger training data set. Additionally, it is operationally desirable to increase the number of RB intervals from the coarse-20% interval that was dictated by the limited amount of Wx data. There is a very significant operational difference in TMU challenge between 23% route blockage and 39% route blockage for a number of these highly congested sectors. Both of these issues will be addressed through an increase in Wx data collection and processing.

5. FUTURE WORK

Currently the exploratory study described above is being expanded to include the following:

1. Automate a data collection process for all ATC sectors within CIWS domain. Given that the CIWS architecture is in place, an algorithm can be developed to collect data whenever active Wx is present within an ATC sector. This will increase the data made available at the now poorly sampled higher RB values and, significantly increase the number of "unorganized" Wx type events. Also, as the number of Wx-route blockage data points increases, the quantization of the route blockage intervals could possibly be decreased. With better sampling of higher RB intervals, more robust pattern classification routines can be applied.
2. Experimental verification of the impact metric RB using actual flight track data. It would be desirable to experimentally validate the individual route blockage scores and the ATC sector blockage

scores as a measure of the sector capacity.

3. Consideration of the time varying usage of the various routes in an ATC sector. Daily demand on the various routes within ATC sectors of the NAS varies considerably. It would be desirable to weight the blockage of various routes in a sector by the fair weather demand. This calculation can significantly reduce the sector blockages that result from Wx impact on routes with little demand or negate blockages that occur on routes that are not in use.

6. REFERENCES

- DeLaura, R., and J. Evans, 2005: *An exploratory study of Modeling Enroute Pilot Convective Storm Flight Deviation Behavior*, 12th Conference on Aviation, Range and Aerospace Meteorology, American Meteorological Society, Atlanta, GA.
- DeLaura, R., and S. Allan, 2003: Route selection decision support in convective weather: a case study of the effects of weather and operational assumptions on departure throughput, 5th Eurocontrol/FAA ATM R&D Seminar ATM-2003, Budapest, Hungary, <http://atm2003.eurocontrol.fr/>
- Histon, J., R.J. Hansman, B. Gottlieb, H. Kleinwaks, S. Yenson, D. Delahaye, S. Peuchmorel, 2002: Structural considerations and cognitive complexity in air traffic control, 21st Digital Avionics Systems Conference, Irvine, CA.
- Huberdeau, M and J. Gentry, 2004: Use of the Collaborative Convective Forecast Product in the Air Traffic Control Strategic Planning Process," ATCA Journal of Air Traffic Control, April-June, pages 9-14.
- Lippmann, R.P. and L. Kukolich, 2004: *LNKnet User's Guide*, MIT Lincoln Laboratory.
- Lippmann, R.P., L. Kukolich, and E. Singer., 1993: *LNKnet Neural Network Machine Learning, and Statistical Software for Pattern Classification*, The Lincoln Laboratory Journal, Vol. 6, Num. 2
- Klinge-Wilson, D. and J. Evans, 2005: *Description of the Corridor Integrated Weather System (CIWS)*, MIT Lincoln Laboratory Project Report ATC-317.
- Mahoney, J.L., J.K. Hederson, B.G. Brown, J.E. Hart, A. Loughe, C. Fischer and B. Sigren, 2002: *The Real-Time Verification System (RTVS) and its Application to Aviation Weather Forecast*, 10th Conference on Aviation, Range, and Aerospace Meteorology, 13-16 May, Portland, OR.
- Mahoney, J., S. Seseske, J. Hart, M. Kay and B. Brown, 2004: *Defining observation fields for*

- verification of spatial forecasts of convection: Part 2*, 11th Conference on Aviation, Range, and Aerospace Meteorology, American Meteorological Society, Hyannis, MA.
- Rhoda, D.A. and Pawlak, M., 1999: *An Assessment of Thunderstorm Penetrations and Deviations by Commercial Aircraft in the Terminal Area*, MIT Lincoln Laboratory, NASA/A-2.
- Rhoda, D., E. Kocab and M. Pawlak, 2002: *Aircraft encounters with Thunderstorms in Enroute vs. Terminal Airspace Above Memphis, Tennessee*, 10th Conference on Aviation, Range, and Aerospace Meteorology, American Meteorological Society, Portland, OR
- Robinson, M., J. Evans, B. Crowe, D. Klingele-Wilson and S. Allan, 2004: *CIWS Operational Benefits 2002-3: Initial Estimates of Convective Weather Delay Reduction*, MIT Lincoln Laboratory Project Report ATC-313